# Critical Quantum Metrology Assisted by Real-Time Feedback Control

Raffaele Salvia,[1,2,*] Mohammad Mehboudi,[2] and Martí Perarnau-Llobet[2,†]
[1]*Scuola Normale Superiore, I-56127 Pisa, Italy*
[2]*Département de Physique Appliquée, Université de Genève, 1211 Genève, Switzerland*

(Received 7 December 2022; revised 27 March 2023; accepted 30 May 2023; published 16 June 2023)

We investigate critical quantum metrology, that is, the estimation of parameters in many-body systems close to a quantum critical point, through the lens of Bayesian inference theory. We first derive a no-go result stating that any nonadaptive strategy will fail to exploit quantum critical enhancement (i.e., precision beyond the shot-noise limit) for a sufficiently large number of particles $N$ whenever our prior knowledge is limited. We then consider different adaptive strategies that can overcome this no-go result and illustrate their performance in the estimation of (i) a magnetic field using a probe of 1D spin Ising chain and (ii) the coupling strength in a Bose-Hubbard square lattice. Our results show that adaptive strategies with real-time feedback control can achieve sub-shot-noise scaling even with few measurements and substantial prior uncertainty.

DOI: 10.1103/PhysRevLett.130.240803

*Introduction.*—Physical systems prepared close to a phase transition are a powerful resource for metrology and sensing applications, as they are extremely sensitive to small variations of certain parameters. This long-standing idea has been recently considered in the quantum regime by exploiting quantum phase transitions in the ground state, or dissipative steady states [1–3], of many-body [4–7] or light-matter interacting systems [8–11]. In this case, quantum fluctuations in the proximity of a quantum critical point can be exploited for quantum-enhanced sensing [12,13].

In a typical protocol in critical quantum metrology, the parameter $\lambda$ to be estimated (e.g., a magnetic field) is encoded in the ground state $\rho(\lambda)$ of a quantum probe. By adiabatically driving the Hamiltonian of the probe close to the critical point, the state $\rho(\lambda)$ becomes highly sensitive to small variations of $\lambda$. This leads to diverging susceptibilities that can be exploited for highly precise parameter estimation [14–16]. More precisely, given an $N$-body probe, the precision $\Delta\lambda$ of the estimation can decay faster than the shot-noise limit $1/\sqrt{N}$ [17,18] when the measurements are performed close to a critical point.

While critical quantum metrology provides an exciting avenue for quantum-enhanced measurements, it also faces important challenges. A notable one is critical slowing down [6], which can be mitigated by appropriate driving schemes [10,19] or alternative approaches [19–22]. A second challenge is that often (almost) perfect prior knowledge of the parameter to be estimated $\lambda$ is needed to exploit the critically enhanced measurement sensitivity, since the critical region $\Delta_c$ shrinks with the system size (see details below) [23]. This may not be seen as a drawback in the framework of local estimation, aiming at measuring the smallest variations around a known parameter, but becomes crucial in global sensing [24], i.e., in scenarios with limited prior knowledge about $\lambda$.

Motivated by the potential use of critical quantum systems in global sensing problems, we find the following two results. First, we derive a no-go theorem stating that nonadaptive schemes are always limited by a shot-noise scaling even in the presence of a quantum phase transition. This can be contrasted to a similar result for the task of estimating temperature in interacting systems [25]; our result is instead applicable to the estimation of any parameter of a quantum ground state. Second, we characterize adaptive schemes that can overcome this bound and reach sub-shot-noise scaling, the level of violation depending directly on the universality class of the phase transition. These schemes are illustrated for the estimation of (i) a magnetic field using as a probe a 1D spin Ising chain and (ii) the hopping term in a Bose-Hubbard square lattice. All our results are obtained within a Bayesian approach [26].

*Preliminaries.*—We seek to estimate an unknown parameter $\lambda \in [\lambda_{\min}, \lambda_{\max}]$, with a prior distribution $p_0(\lambda)$. We consider $m$ consecutive measurements of the ground state $\rho(\lambda, \vec{s})$ of an $N$-body interacting system described by a Hamiltonian $\hat{H}(\lambda, \vec{s})$. Besides $\lambda$, $\hat{H}(\lambda, \vec{s})$ also depends on externally controllable parameters $\vec{s}$, which can be modified to enhance sensitivity during measurements. In our analysis, the relevant resources are the number of particles $N$ and the total number of measurements implemented $m$.

The $k$th measurement on the system can be described by a positive operator-valued measure, with elements $\Pi_x^{(k)} \geq 0$ satisfying $\int dx \Pi_x^{(k)} = \mathbb{I}$, with $\mathbb{I}$ the identity operator. Let $\vec{x}_k = \{x_1, \ldots, x_k\}$ denote the register of the outcomes of the first $k$ measurements and $p(\lambda|\vec{x}_k)$ the posterior distribution—for a lighter notation, we drop the dependence of the posterior on the setting $\vec{s}_k$. The posterior distribution is updated according to Bayes' rule [27]:

$$p(\lambda|\vec{x}_k) = \frac{p(x_k|\lambda,\vec{s}_k)p(\lambda|\vec{x}_{k-1})}{p(x_k|\vec{x}_{k-1},\vec{s}_k)} \tag{1}$$

with $k = 1,\ldots,m$. Here, $p(\lambda|x_0) \equiv p_0(\lambda)$, and $p(x_k|\lambda,\vec{s}_k) = \mathrm{Tr}[\Pi_{x_k}^{(k)}\rho(\lambda,\vec{s}_k)]$ is the probability that in the $k$th measurement we observe the outcome $x_k$ when the control parameters are tuned to $\vec{s}_k$. Note that in adaptive strategies the control parameters generally depend on the observed outcomes. Finally, $p(x_k|\vec{x}_{k-1},\vec{s}_k) = \int d\lambda p(x_k|\lambda,\vec{s}_k)p(\lambda|\vec{x}_{k-1})$ is the normalization factor.

After each measurement, one builds an estimator $\tilde{\lambda}_k$ that assigns an estimate value to the unknown parameter according to the observed data. To quantify the estimation error, we use the standard *expected mean square distance* (EMSD) as our figure of merit [28,29]—we expect that our main conclusions hold for other reasonable choices of the error function. After performing $m$ measurements, it reads

$$\mathrm{EMSD} \coloneqq \int d\lambda p_0(\lambda)\int d\vec{x}_m p(\vec{x}_m|\lambda)[\tilde{\lambda}(\vec{x}_m)-\lambda]^2. \tag{2}$$

The EMSD can be bounded via two complementary approaches:

$$\mathrm{EMSD} \geq \left[F_0 + \int d\lambda p_0(\lambda)\mathcal{F}[p(\vec{x}_m|\lambda)]\right]^{-1}, \tag{3a}$$

$$\mathrm{EMSD} \geq \int d\lambda p_0(\lambda)\mathcal{F}[p(\vec{x}_m|\lambda)]^{-1} \qquad (\text{unb. est.}). \tag{3b}$$

The first bound (3a) follows from the Van Trees inequality and is valid for any estimator [30,31]. On the other hand, Eq. (3b) is a direct consequence of the Cramér-Rao bound [32] and is, hence, valid only for unbiased estimators $\tilde{\lambda}_{\mathrm{ub}}$ for which $\int d\vec{x}_m p(\vec{x}_m|\lambda)\tilde{\lambda}_{\mathrm{ub}}(\vec{x}_m) = \lambda$. Here, $F_0 \coloneqq \int d\lambda p_0(\lambda)[\partial_\lambda \log p_0(\lambda)]^2$ is a functional of *only* the prior information, while

$$\begin{aligned}\mathcal{F}[p(\vec{x}_m|\lambda)] &\coloneqq \int d\vec{x}_m p(\vec{x}_m|\lambda)[\partial_\lambda \log p(\vec{x}_m|\lambda)]^2 \\ &= \sum_{k=1}^{m}\int d\vec{x}_{k-1}p(x_{k-1}|\lambda,\vec{s}_{k-1})\mathcal{F}[p(x_k|\lambda,\vec{s}_k)]\end{aligned} \tag{4}$$

is the classical Fisher information of the trajectory characterized by $p(\vec{x}_m|\lambda)$. From the quantum Cramér-Rao bound, we know that

$$\mathcal{F}[p(x_k|\lambda,\vec{s})] \leq \mathcal{F}^{\mathrm{Q}}(\lambda,\vec{s}), \tag{5}$$

where $\mathcal{F}^{\mathrm{Q}}(\lambda,\vec{s})$ is the quantum Fisher information (QFI), the maximum Fisher information over all possible measurements [33–35].

The appearance of the QFI in the lower bounds of the EMSD enables us to connect the Bayesian approach with previous results in critical quantum metrology obtained within a frequentist framework, where the divergence of $\mathcal{F}^{\mathrm{Q}}(\lambda,\vec{s}_k)$ close to a phase transition is exploited [4–7]. In particular, we are concerned with systems which exhibit a second-order quantum phase transition [36]. This means that, in the thermodynamic limit ($N\to\infty$), the energy of the ground state of $\hat{H}(\lambda,\vec{s})$ has a nonanalyticity point at some value $\lambda_c(\vec{s})$. Close to the critical point $\lambda_c(\vec{s})$, the behavior of the system is described by power laws with a set of *critical exponents* which do not depend upon the microscopic details of the Hamiltonian but only on its *universality class* [37]. In particular, the correlation length $\xi$ of the system diverges as $\xi \sim (\lambda-\lambda_c)^{-\nu}$ for some critical exponent $\nu$ [38]. The theory of finite size scaling [39–41] is based on the hypothesis that $\xi$ is the most relevant length scale in the proximity of the critical point $\lambda_c(\vec{s})$. For a system with spacial dimension $d$, which has a finite size $L = N^{1/d}$, the critical region of the phase diagrams occurs when $\xi \gg L$. This implies that the system is critical when

$$|\lambda-\lambda_c| \leq CN^{-1/d\nu} \eqqcolon \Delta_c \tag{6}$$

for some constant $C$ which does not depend on $N$. Here, we define $\Delta_c$ as the width of the critical region, which shrinks as $\Delta_c \propto N^{-1/d\nu}$.

Inside the critical region, the universal part of the QFI is expected to behave as [6,42]

$$\mathcal{F}^{\mathrm{Q}}(\lambda_c(\vec{s});\vec{s}) \approx \alpha_c N^{2/d\nu}, \qquad |\lambda-\lambda_c| \leq \Delta_c, \tag{7}$$

where $\alpha_c$ is some constant that is independent of $N$. When $d\nu < 2$, the universal term (7) becomes the leading term of the QFI, and the system-specific corrections [43] become subleading [44,45]. Outside the critical region, the superlinear scaling of the QFI is lost and the universal contribution to the QFI behaves as $\mathcal{F}^{\mathrm{Q}}(\lambda,\vec{s}) \approx N|\lambda-\lambda_c(\vec{s})|^{d\nu-2}$ [14]. More generally, we can bound the QFI by a linear function of $N$:

$$\mathcal{F}^{\mathrm{Q}}(\lambda_c(\vec{s});\vec{s}) \leq \alpha_{nc}N, \qquad |\lambda-\lambda_c| \geq \Delta_c, \tag{8}$$

for some constant $\alpha_{nc}$ independent of $N$.

*Fundamental bounds in Bayesian critical quantum metrology: Adaptive vs nonadaptive protocols.*—Let us now characterize the limitations arising due to the prior uncertainty $p_0(\lambda)$. First of all, we can find an upper bound on EMSD, which is independent of $p_0(\lambda)$. Using $\max_\lambda \mathcal{F}^{\mathrm{Q}}(\lambda,\vec{s}) \approx \alpha_c N^{2/d\nu}$, by combining Eqs. (3a) and (5) we obtain in the large $N$ limit

$$\mathrm{EMSD} \gtrsim [m\alpha_c N^{2/d\nu}]^{-1}. \tag{9}$$

Saturating this lower bound requires feedback control. Indeed, let us consider nonadaptive strategies in which the control parameters $\vec{s}_k$ are fixed to some initial value $\vec{s}_0$ and do not depend on the measurement outcomes. Focusing on unbiased estimators and combining Eqs. (5) and (3b), we obtain

$$\begin{aligned}\mathrm{EMSD} &\overset{\text{nonadaptive}}{\geq} \int d\lambda p_0(\lambda)[m\mathcal{F}^{\mathrm{Q}}(\lambda,\vec{s}_0)]^{-1} \\ &= \left(\int_{|\lambda-\lambda_c|>\Delta_c} + \int_{|\lambda-\lambda_c|\leq\Delta_c}\right) d\lambda \frac{p_0(\lambda)}{m\mathcal{F}^{\mathrm{Q}}(\lambda,\vec{s}_0)} \\ &\geq \frac{P_0^{\mathrm{nc}}}{m\alpha_{nc}N} + \mathcal{O}(N^{-2/d\nu}) \qquad (10)\end{aligned}$$

where in the second line above we separated the contributions of critical and noncritical regions and in the last line we used Eq. (8) and defined $P_0^{\mathrm{nc}} \coloneqq \int_{|\lambda-\lambda_c|\geq\Delta_c} d\lambda p_0(\lambda)$, the prior probability of being outside the critical region. Except the extreme case of perfect *a priori* knowledge [in which $p_0(\lambda)$ is a delta distribution at the true value], we have $P_0^{\mathrm{nc}} > 0$ for sufficiently large $N$ because $\Delta_c \propto N^{-1/d\nu}$. Therefore, for any practical estimation process with finite uncertainty on the estimated parameter, nonadaptive estimation methods in critical metrology are eventually limited by a shot-noise scaling. Recall that Eq. (10) has been obtained under the assumption of an unbiased estimator, which we expect in the asymptotic limit of a large amount of measurements. In Supplemental Material [46] (with Refs. [47–57]), we generalize this no-go result to arbitrary estimators exploiting instead the bound (3a).

*Adaptive strategies.*—We now discuss two feedback-based protocols that can overcome the no-go bound and achieve superlinear precision: (I) a standard two-step adaptive process [58,59] and (II) a real-time adaptive control, where the control parameters $\vec{s}$ are continuously updated.

Let us consider $m$ total measurements. In the two-step adaptive protocol (I), one first performs $\epsilon m$ (with $\epsilon \ll 1$) identical measurements for some configuration $\vec{s}_1$ that can be chosen according to $p_0(\lambda)$. An estimate $\tilde{\lambda}$ is then obtained. In a second step, one measures the remaining $(1-\epsilon)m$ copies for a configuration satisfying $\lambda_c(\vec{s}) = \tilde{\lambda}$; that is, one prepares the system at criticality assuming that $\tilde{\lambda}$ is the true parameter. For this approach to work, we need that after the first step the posterior distribution is fully concentrated in the critical region. That is, $\delta < \Delta_c$, where $\delta \propto (\epsilon m N)^{-1/2}$ is the width of the posterior distribution, which implies $m \gg N^{(2/d\nu)-1}$. This can be demanding in many-body systems, as $d\nu < 2$ for critically enhanced metrology.

To exploit criticality in regimes where $m < N$, we consider (II) real-time feedback control. In this case, at each step $k$ an estimate $\tilde{\lambda}_k$ is built, and the control parameters are chosen according to $\lambda_c(\vec{s}_k) = \tilde{\lambda}_k$. As we now show, this strategy turns out to be crucial to exploit critically enhanced sensing.

*(i) Magnetometry in the one-dimensional transverse Ising model.*—With $d\nu = 1$ and its QFI scaling as $N^2$ at criticality [16,42,60], this model has been widely used for critical metrology with focus on the asymptotic limit where the same measurement is repeated a large number of times (via a frequentist approach) [5,7]. Here, instead, we consider adaptive schemes given a small number of measurements within a Bayesian approach.

The Hamiltonian reads (with periodic boundary conditions)

$$\hat{H}(h;s) = J\sum_{i=1}^{N} \hat{\sigma}_i^x \hat{\sigma}_{i+1}^x + (h+s)\sum_{i=1}^{N} \hat{\sigma}_i^z, \qquad (11)$$

which can be diagonalized using the Jordan-Wigner and the Fourier transformation. At the ground state $\rho(h;s)$, the system undergoes a quantum phase transition when $s = s_c(h) = J/2 - h$.

We consider the estimation of the fixed magnetic field $h$ and assume that we can apply an additional controllable magnetic field $s$ parallel to $h$. We infer $h$ through projective measurements of the transverse magnetization $\hat{M}_z = \frac{1}{2}\sum_{i=1}^{N} \hat{\sigma}_i^z$. This is not the optimal measurement: While the QFI scales as $N^2$, the Fisher information for the $M_z$ measurement grows at a more modest $\sim N^{1.5}$ (see Supplemental Material [46]). An outcome $x_k$ is observed with probability

$$p(x_k|h,s_k) = \mathrm{Tr}[\rho(h,s_k)\Pi_{x_k}], \quad x_k \in \{0, \pm 1/2, \ldots, \pm N/2\}, \qquad (12)$$

where $\Pi_{x_k}$ is the projector over the eigenspace of $\hat{M}_z$ with eigenvalue $x_k$.

Although our results are not limited by the choice of the prior, we initially set it to

$$p_0(h) = \frac{\exp\left[\alpha \sin^2\left(\pi \frac{h-h_{\min}}{h_{\max}-h_{\min}}\right)\right] - 1}{(h_{\max}-h_{\min})[e^{\alpha/2} I_0(\alpha/2) - 1]}, \qquad (13)$$

where $I_0$ is the order-zero modified Bessel function of the first kind. In our simulations we take $\alpha = -100$ which looks like a flat distribution, but smoothly vanishes at the borders $p_0(h_{\min}/h_{\max}) = 0$ [61].

In Fig. 1, we depict how the posterior evolves for a particular measurement trajectory of the adaptive and nonadaptive schemes. It illustrates how the adaptive protocol converges to the true value much faster than the nonadaptive one. To quantify this difference, we plot the EMSD in Fig. 2. We observe that adaptive strategies can outperform arbitrary nonadaptive protocols (including

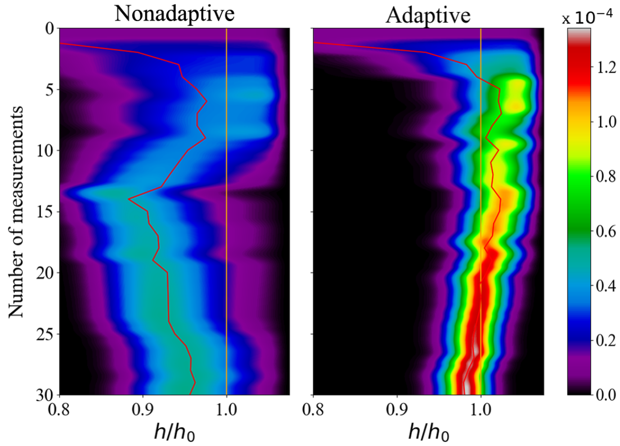


FIG. 1. Simulation of a single trajectory in estimation of the magnetic field in the Ising model. The parameter is fixed to $h_0$ throughout, while our belief on its value is given by the prior $p(h)$ which we update to the posterior $p(h|\vec{x}_k)$ (contour plot) according to the data collected by measuring the magnetization, i.e., $\vec{x}_k$ for both nonadaptive (left) and adaptive (right) scenarios. The vertical line shows the true parameter value, while the fluctuating line is the estimated parameter. Here, we set $N = 40$, $h_0 = 1.3$, while $h_{\rm min} = 0.6$, $h_{\rm max} = 1.4$, $\alpha = -100$, and $J = 1$.

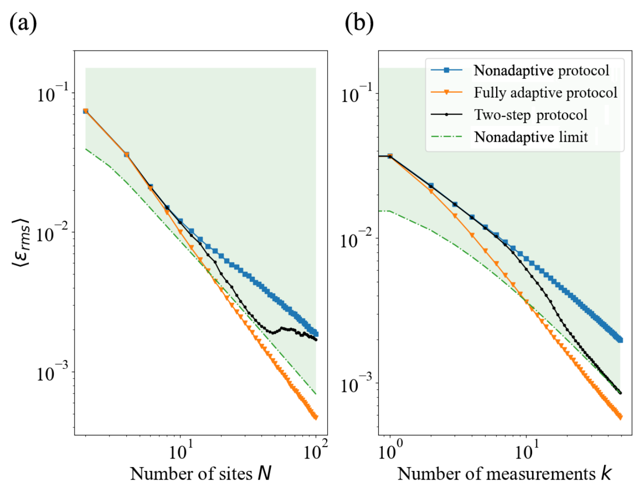


FIG. 2. Log-log plot of EMSD in estimation of $h$ in the Ising model. This is obtained by a Monte Carlo simulation of the measurement procedure for many different values of $h$ sampled from the prior distribution. Again, we are measuring the transverse magnetization. Only the green region is potentially accessible by nonadaptive strategies which is computed via the lower bound Eq. (3a) with the optimal measurement Eq. (5). In the nonadaptive protocol, the magnetization is measured by fixing the field to the one that minimizes the EMSD for an immediate measurement that follows. In the two-step protocol, the field is adjusted exactly once, when the width of the posterior becomes smaller than $\Delta_c = 3/N^{d\nu}$. In the fully adaptive protocol, the applied field can be adjusted after every measurement. The curves are calculated by averaging over 10 000 trajectories like the one shown in Fig. 1. In (a), we set $m = 24$, and $h_0$ is randomly sampled according to Eq. (13) with $\alpha = -100$, $h_{\rm min} = 0.6$, and $h_{\rm max} = 1.4$. The same parameters are used for (b), where we vary the number of measurements while setting $N = 40$.

optimal measurements maximizing the QFI), which are limited by a shot-noise scaling. In particular, with adaptivity we reach EMSD $\propto N^{1.5}$ even for a small number of measurements $m = 24$. When $N$ is instead fixed, noticeable advantages are also observed as a function of $m$.

*(ii) The two-dimensional bosonic Hubbard model.*—As a second example, we consider the system of repulsing bosonic particles hopping through a lattice [62], which undergoes a transition from the superfluid phase to the Mott insulator phase. The simplest model that captures this system is the Bose-Hubbard Hamiltonian

$$\hat{H}(t;U) = -t\sum_{\langle i,j\rangle}\hat{a}_i^\dagger\hat{a}_j + \frac{U}{2}\hat{n}_i(\hat{n}_i - 1) - \mu\sum_i \hat{n}_i, \quad (14)$$

where $\hat{a}_i^\dagger$ and $\hat{a}_i$ are bosonic creation and annihilation operators, respectively, on the $i$th site, $\hat{n}_i = \hat{a}_i^\dagger\hat{a}_i$, and the first sum runs over the neighboring sites.

We aim at estimating the hopping coupling $t$ and take the on-site repulsion coupling $U$ as our control parameter. For instance, in an implementation of the model in Josephson junctions [63–70], controlling $U$ is possible by tuning the capacitance of the junctions. We fix the chemical potential to $\mu = 1/2$. In a square 2D grid with closed boundary conditions, the system undergoes a second-order phase transition when $t = t_C \simeq 0.06U$ [71]. The critical exponent is $\nu \simeq 0.67$ [72,73], which by using Eq. (7) gives $\mathcal{F}^{\rm Q}(t,U) \propto N^{1.34}$ at the critical region.

To estimate $t$, we measure the *superfluid density* of the lattice $\rho_s$. This is a practical measurement; e.g., in granular superconductors [74], it can be experimentally measured through the magnetic penetration depth of the lattice [75]. A standard finite size scaling argument predicts that near the critical region

$$\rho_s = N^{-1/2}g[(t - t_C)N^\nu], \quad (15)$$

where $g$ is a universal function; i.e., its output is independent of $N$. This behavior is fairly preserved at temperatures lower than $T = 0.05U$ (see Fig. S4 in Supplemental Material [46]).

In what follows, we assume that the superfluid density can be measured with shot-noise error in both critical and noncritical regions. More specifically, the outcomes of measuring $\rho_s$ follow a normal distribution

$$p(x|t,U) = \sqrt{\frac{N}{2\pi\sigma_0^2}}\exp\left[-N\frac{[x - \rho_s(t;U)]^2}{2\sigma_0^2}\right], \quad (16)$$

for some constant $\sigma_0$. This leads to a linear QFI with respect to the stiffness parameter, i.e., $\mathcal{F}(\rho_s, U) \propto N$. Using the parameter conversion relation [76], one finds the QFI of the hopping parameter at the critical region:

$$\mathcal{F}(t,U) = (\partial_t\rho_s)^2\mathcal{F}(\rho_s,U) \propto N^{1+2\alpha}, \quad (17)$$

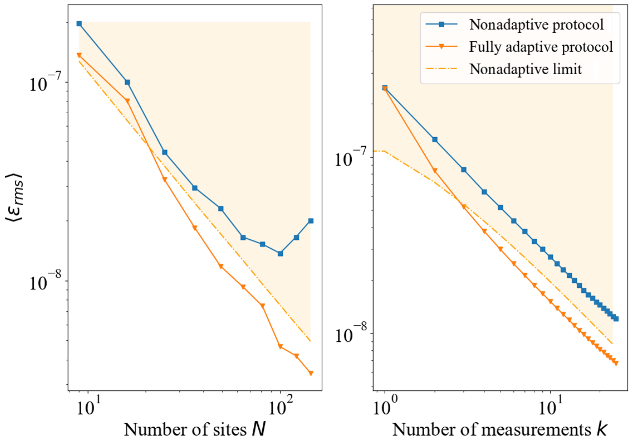


FIG. 3. EMSD for estimation of the hopping parameter $t$ via measuring the superfluid stiffness $\rho_s$ against the lattice size $N$ (left plot) or the number of measurements $k$ (right plot), averaged over 60 000 measurement trajectories, with the starting prior as in Eq. (13). Here, we set $\alpha = -100$, $t_{\min} = 0.054$, $t_{\max} = 0.09$, and $\sigma_0 = 0.01$. For the left plot, the number of measurements is fixed as $m = 16$. For the right plot, the size of the square lattice is fixed at $N = 64$.

with $\alpha = \nu - 1/2 \simeq 0.17$, hence enabling sensing beyond shot noise.

In Fig. 3, we compare the EMSD for optimized adaptive (with real-time feedback control) and nonadaptive protocols. While, in the latter case, the error decreases as $\sim N^{-1}$, the former decreases faster with $\sim N^{-1.34}$ as described by Eq. (17).

*Conclusions.*—In this work, we characterized the relevance of feedback control in critical quantum metrology. Our no-go result shows that nonadaptive protocols are shot-noise limited and highlights the crucial role of feedback control and adaptivity [77–85] in critical quantum metrology. We also investigated two adaptive schemes capable of overcoming this no-go result: a two-step adaptive protocol [58,59] and a fully adaptive protocol where the control parameters are updated after each measurement. The latter was shown to be highly preferable for the examples considered, being capable of reaching sub-shot-noise scaling even given a few measurements and limited prior knowledge.

While we have focused on many-body systems, future work includes investigating similar feedback-based protocols in the context of finite-component quantum phase transitions [10,11,19,86–88]. The performance of more sophisticated feedback protocols [81,89–92] is also worth investigating in the future.

We acknowledge the Swiss National Science Foundation for financial support through the Ambizione Grant No. PZ00P2-186067 and the NCCR SwissMAP.

*raffaele.salvia@sns.it
†marti.perarnaullobet@unige.ch

[1] L. Banchi, P. Giorda, and P. Zanardi, Phys. Rev. E **89**, 022102 (2014).
[2] K. Macieszczak, M. Guţă, I. Lesanovsky, and J. P. Garrahan, Phys. Rev. A **93**, 022103 (2016).
[3] U. Marzolino and T. Prosen, Phys. Rev. B **96**, 104402 (2017).
[4] P. Zanardi, M. G. A. Paris, and L. C. Venuti, Phys. Rev. A **78**, 042105 (2008).
[5] C. Invernizzi, M. Korbman, L. C. Venuti, and M. G. A. Paris, Phys. Rev. A **78**, 042106 (2008).
[6] M. M. Rams, P. Sierant, O. Dutta, P. Horodecki, and J. Zakrzewski, Phys. Rev. X **8**, 021022 (2018).
[7] I. Frérot and T. Roscilde, Phys. Rev. Lett. **121**, 020402 (2018).
[8] M. Bina, I. Amelio, and M. G. A. Paris, Phys. Rev. E **93**, 052118 (2016).
[9] S. Fernández-Lorenzo and D. Porras, Phys. Rev. A **96**, 013817 (2017).
[10] L. Garbe, M. Bina, A. Keller, M. G. A. Paris, and S. Felicetti, Phys. Rev. Lett. **124**, 120504 (2020).
[11] T. Ilias, D. Yang, S. F. Huelga, and M. B. Plenio, PRX Quantum **3**, 010354 (2022).
[12] V. Giovannetti, Science **306**, 1330 (2004).
[13] V. Giovannetti, S. Lloyd, and L. Maccone, Nat. Photonics **5**, 222 (2011).
[14] L. C. Venuti and P. Zanardi, Phys. Rev. Lett. **99**, 095701 (2007).
[15] W.-L. You, Y.-W. Li, and S.-J. Gu, Phys. Rev. E **76**, 022101 (2007).
[16] B. Damski and M. M. Rams, J. Phys. A **47**, 025303 (2013).
[17] W. Schottky, Ann. Phys. (Berlin) **362**, 541 (1918).
[18] P. Hariharan, *Basics of Interferometry* (Academic Press, Boston, 1992).
[19] Y. Chu, S. Zhang, B. Yu, and J. Cai, Phys. Rev. Lett. **126**, 010502 (2021).
[20] K. Gietka, F. Metz, T. Keller, and J. Li, Quantum **5**, 489 (2021).
[21] L. Garbe, O. C. Abah, S. Felicetti, and R. Puebla, Quantum Sci. Technol. **7**, 035010 (2022).
[22] K. Gietka, L. Ruks, and T. Busch, Quantum **6**, 700 (2022).
[23] M. E. Fisher and M. N. Barber, Phys. Rev. Lett. **28**, 1516 (1972).
[24] V. Montenegro, U. Mishra, and A. Bayat, Phys. Rev. Lett. **126**, 200501 (2021).
[25] M. Mehboudi, M. R. Jørgensen, S. Seah, J. B. Brask, J. Kołodyński, and M. Perarnau-Llobet, Phys. Rev. Lett. **128**, 130502 (2022).
[26] U. von Toussaint, Rev. Mod. Phys. **83**, 943 (2011).
[27] T. Bayes and R. Price, Phil. Trans. R. Soc. London **53**, 370 (1763).
[28] H. L. Van Trees and K. L. Bell, J. Acoust. Soc. Am. **123**, 2459 (2008).
[29] S. M. Kay, *Fundamentals of Statistical Signal Processing: Estimation Theory* (Prentice-Hall, Englewood Cliffs, NJ, 1993).
[30] H. Van Trees, *Detection, Estimation, and Modulation Theory* (Wiley, New York, 1968).

[31] R. D. Gill and B. Y. Levit, Bernoulli **1**, 59 (1995).
[32] H. Cramér, *Mathematical Methods of Statistics* (Princeton University Press, Princeton, NJ, 1999), Vol. 26.
[33] S. L. Braunstein and C. M. Caves, Phys. Rev. Lett. **72**, 3439 (1994).
[34] A. S. Kholevo, *Probabilistic and Statistical Aspects of Quantum Theory* (Scuola Normale Superiore, Pisa, 2011).
[35] D. Petz and C. Ghinea, in *Quantum Probability and Related Topics* (World Scientific, Singapore, 2011).
[36] S. Sachdev, *Quantum Phase Transitions* (Cambridge University Press, Cambridge, New York, 2011).
[37] S.-k. Ma, *Modern Theory of Critical Phenomena* (Perseus, Cambridge, MA, 2000).
[38] A. Altland, *Condensed Matter Field Theory* (Cambridge University Press, Leiden, 2010).
[39] C. Domb, *Phase Transitions and Critical Phenomena* (Academic Press, London, 1972).
[40] E. Brézin, J. Phys. (Les Ulis, Fr.) **43**, 15 (1982).
[41] V. Privman, *Finite Size Scaling and Numerical Simulation of Statistical Systems* (World Scientific, Singapore, 1990).
[42] A. F. Albuquerque, F. Alet, C. Sire, and S. Capponi, Phys. Rev. B **81**, 064418 (2010).
[43] D. Schwandt, F. Alet, and S. Capponi, Phys. Rev. Lett. **103**, 170501 (2009).
[44] A. Polkovnikov and V. Gritsev, in *Understanding Quantum Phase Transitions* (CRC Press, Boca Raton, 2010), pp. 59–90.
[45] C. De Grandi, V. Gritsev, and A. Polkovnikov, Phys. Rev. B **81**, 012303 (2010).
[46] See Supplemental Material at http://link.aps.org/supplemental/10.1103/PhysRevLett.130.240803 for critical quantum metrology assisted by real-time feedback control, which includes Refs. [47–57].
[47] S.-J. GU, Int. J. Mod. Phys. B **24**, 4371 (2010).
[48] H. Lee, S. Fang, and D.-W. Wang, Phys. Rev. A **95**, 053622 (2017).
[49] A. Savitzky and M. J. E. Golay, Anal. Chem. **36**, 1627 (1964).
[50] L. P. Pitaevskiĭ and S. Stringari, *Bose-Einstein Condensation and Superfluidity* (Oxford University Press, Oxford, 2016).
[51] J. Bardeen, Phys. Rev. Lett. **1**, 399 (1958).
[52] E. Guadagnini, J. Stat. Mech. (2017) 073104.
[53] N. V. Prokof'ev and B. V. Svistunov, Phys. Rev. B **61**, 11282 (2000).
[54] M. E. Fisher, M. N. Barber, and D. Jasnow, Phys. Rev. A **8**, 1111 (1973).
[55] N. Byers and C. N. Yang, Phys. Rev. Lett. **7**, 46 (1961).
[56] O. Simard, C.-D. Hébert, A. Foley, D. Sénéchal, and A.-M. S. Tremblay, Phys. Rev. B **100**, 094506 (2019).
[57] A. Paramekanti, N. Trivedi, and M. Randeria, Phys. Rev. B **57**, 11639 (1998).
[58] O. E. Barndorff-Nielsen and R. D. Gill, J. Phys. A **33**, 4481 (2000).
[59] A. Luati, Ann. Stat. **32**, 1770 (2004).
[60] B. Damski, Phys. Rev. E **87**, 052131 (2013).
[61] Y. Li, L. Pezzè, M. Gessner, Z. Ren, W. Li, and A. Smerzi, Entropy **20**, 628 (2018).
[62] M. P. A. Fisher, P. B. Weichman, G. Grinstein, and D. S. Fisher, Phys. Rev. B **40**, 546 (1989).
[63] R. M. Bradley and S. Doniach, Phys. Rev. B **30**, 1138 (1984).
[64] H. S. J. van der Zant, F. C. Fritschy, W. J. Elion, L. J. Geerligs, and J. E. Mooij, Phys. Rev. Lett. **69**, 2971 (1992).
[65] A. van Oudenaarden and J. E. Mooij, Phys. Rev. Lett. **76**, 4947 (1996).
[66] E. Chow, P. Delsing, and D. B. Haviland, Phys. Rev. Lett. **81**, 204 (1998).
[67] D. Jaksch, C. Bruder, J. I. Cirac, C. W. Gardiner, and P. Zoller, Phys. Rev. Lett. **81**, 3108 (1998).
[68] M. Greiner, O. Mandel, T. Esslinger, T. W. Hänsch, and I. Bloch, Nature (London) **415**, 39 (2002).
[69] Y. Yanay, J. Braumüller, S. Gustavsson, W. D. Oliver, and C. Tahan, npj Quantum Inf. **6**, 58 (2020).
[70] J. Yu, E. Lauricella, M. Elsayed, K. Shepherd, N. S. Nichols, T. Lombardi, S. W. Kim, C. Wexler, J. M. Vanegas, T. Lakoba, V. N. Kotov, and A. Del Maestro, Phys. Rev. B **103**, 235414 (2021).
[71] B. Capogrosso-Sansone, Ş. G. Söyler, N. Prokof'ev, and B. Svistunov, Phys. Rev. A **77**, 015602 (2008).
[72] M. Hasenbusch, Phys. Rev. B **100**, 224517 (2019).
[73] S. M. Chester, W. Landry, J. Liu, D. Poland, D. Simmons-Duffin, N. Su, and A. Vichi, J. High Energy Phys. 06 (2020) 142.
[74] G. Deutscher, J. Supercond. Novel Magn. **34**, 1699 (2021).
[75] Y. J. Uemura, L. P. Le, G. M. Luke, B. J. Sternlieb, W. D. Wu, J. H. Brewer, T. M. Riseman, C. L. Seaman, M. B. Maple, M. Ishikawa, D. G. Hinks, J. D. Jorgensen, G. Saito, and H. Yamochi, Phys. Rev. Lett. **66**, 2665 (1991).
[76] M. G. Paris, Int. J. Quantum. Inform. **07**, 125 (2009).
[77] D. W. Berry and H. M. Wiseman, Phys. Rev. Lett. **85**, 5098 (2000).
[78] M. A. Armen, J. K. Au, J. K. Stockton, A. C. Doherty, and H. Mabuchi, Phys. Rev. Lett. **89**, 133602 (2002).
[79] H. M. Wiseman and G. J. Milburn, *Quantum Measurement and Control* (Cambridge University Press, Cambridge, England, 2009).
[80] G. Y. Xiang, B. L. Higgins, D. W. Berry, H. M. Wiseman, and G. J. Pryde, Nat. Photonics **5**, 43 (2010).
[81] A. Hentschel and B. C. Sanders, Phys. Rev. Lett. **107**, 233601 (2011).
[82] A. Serafini, ISRN Optics **2012**, 1 (2012).
[83] C. Bonato, M. S. Blok, H. T. Dinani, D. W. Berry, M. L. Markham, D. J. Twitchen, and R. Hanson, Nat. Nanotechnol. **11**, 247 (2015).
[84] R. Demkowicz-Dobrzański, J. Czajkowski, and P. Sekatski, Phys. Rev. X **7**, 041009 (2017).
[85] A. Lumino, E. Polino, A. S. Rab, G. Milani, N. Spagnolo, N. Wiebe, and F. Sciarrino, Phys. Rev. Appl. **10**, 044033 (2018).
[86] R. Puebla, M.-J. Hwang, J. Casanova, and M. B. Plenio, Phys. Rev. Lett. **118**, 073001 (2017).
[87] L. Garbe, arXiv:2011.01995.
[88] R. D. Candia, F. Minganti, K. V. Petrovnin, G. S. Paraoanu, and S. Felicetti, npj Quantum Inf. **9**, 23 (2023).

[89] A. Hentschel and B. C. Sanders, Phys. Rev. Lett. **104**, 063603 (2010).
[90] N. B. Lovett, C. Crosnier, M. Perarnau-Llobet, and B. C. Sanders, Phys. Rev. Lett. **110**, 220501 (2013).
[91] S. Nolan, A. Smerzi, and L. Pezzè, npj Quantum Inf. **7**, 169 (2021).
[92] A. Fallani, M. A. C. Rossi, D. Tamascelli, and M. G. Genoni, PRX Quantum **3**, 020310 (2022).